Magnetic properties of fcc iron in Fe - Pt nano-scale multilayers

Magnetic properties of fcc iron in Fe–Pt nano-scale multilayers

M Zhang†, F Pan†‡ and B X Liu†‡

† Department of Materials Science and Engineering, Tsinghua University, 100084, People's Republic of China
‡ Centre of Condensed Matter and Radiation Physics, CCAST (World Laboratory), Beijing 100080, People's Republic of China

Abstract. The vapour-deposition technique was employed to grow Fe–Pt multilayers at a deposition rate of 0.01–0.02 nm s^{-1}. The thickness, periodicity, chemical composition, microstructure, and magnetic moment of the films were characterized and measured by various methods. It was found that, when the Fe layers were thinner than 3.4 nm, the Fe atoms grew in an fcc structure on the polycrystalline fcc Pt layers with a fixed thickness of 7.0 nm. The fcc Fe in the Fe–Pt multilayers exhibits ferromagnetic behaviour, and its magnetic moment can be as high as $2.12\mu_B$. The possible mechanism responsible for the modification of magnetic properties of fcc Fe is discussed.

1. Introduction

In the last few years, magnetic multilayer thin films on a nanometre scale with artificial periodicity (modulated structure) have attracted much attention because these films may feature some anomalous magnetic properties, such as changes in magnetization as the magnetic layer thickness is reduced, appearance in some cases of a uniaxial interfacial anisotropy, and giant magnetoresistance. These phenomena are probably related to the existence of surface and interface states, i.e., the reduced coordination number and symmetry of atoms in the surface, transitional structure sublayer, interface roughness, associated chemical disordering, etc [1–3]. Based on an all-electron total energy local spin density approach, Freeman and coworkers [4–6] predicted that there would be a significant enhancement in two-dimensional magnetism at surfaces and interfaces in transition metals grown on noble metals, e.g., Fe in a thin-film form with fcc structure can exhibit ferromagnetic behaviour, in contrast to its bulk fcc phase, which is non-magnetic. The magnetic moment of the Fe atom, in comparison to its value of $2.15\mu_B$ in the bcc bulk, could be up to $2.98\mu_B$ for the topmost Fe overlayer and the clean Fe (001) surface. Spin-polarized layer Korringa–Kohn–Rostoker method investigations in superlattices and interfaces by MacLaren *et al* [7, 8], and tight-binding calculations of the magnetic properties of surface, interface and multilayers by Krompiewski *et al* [2], Tersoff and Falicov [9], and Falicov *et al* [10] gave a similar prediction. In our recent studies [3, 11, 12] electron-beam vapour deposition was employed to prepare Fe–noble metal (Cu, Au, Ag, Pd) modulated thin films, and the magnetic moment per Fe atom was enhanced significantly with decreasing Fe layer thickness (t_{Fe}) in multilayers with fixed thickness of noble metal layers. For

instance, in Fe–Cu and Fe–Pd multilayers, the magnetic enhancement may be attributed to the formation of metastable fcc Fe emerging in these films, in contrast to the paramagnetic behaviour of the bulk fcc phase. Very recently, Koide *et al* [13] obtained an fcc phase in Fe (0.47 nm)–Pt (1.85 nm) 80-bilayer films by radio-frequency sputtering with two targets. It is therefore of interest to study Fe–Pt nano-multilayers to see whether Fe can grow in an fcc structure with modified magnetic properties. In this paper, we report experimental results of magnetic properties of fcc Fe observed in Fe–Pt multilayers prepared in an electron-beam vapour deposition system. Correlation between magnetic properties and microstructure as well as the possible mechanism responsible for these magnetic phenomena is also discussed.

2. Experimental procedure

The Fe–Pt multilayer films were prepared by alternately depositing pure iron (99.99%) and pure platinum (99.99%) at a rate of 0.01–0.02 nm s^{-1} onto glass substrates 0.1 mm thick (for magnetic property measurement) and NaCl single-crystal chips with a freshly cleaved surface (for microstructure studies) in an ultra-high-vacuum electron-gun evaporation system at a vacuum level of 2×10^{-6} Pa. The thickness of the Pt layers (t_{Pt}) was fixed at 7.0 nm and the Fe layer thickness varied from 1.2 to 8.0 nm, controlled by a quartz monitor in the system. The total thickness of the films was approximately 150 nm. Samples were analysed by high-energy electron microscopy (HEEM), selected area electron diffraction (SAD), and x-ray diffraction to identify the structure. Rutherford backscattering (RBS) was also employed to measure the thickness, periodicity, and composition of the samples. The magnetic properties were measured with a vibrating-sample magnetometer (VSM), with a resolution of 5×10^{-6} emu, in a magnetic field of up to 10 kOe at room temperature. The size of the VSM samples was 4 mm $\times$ 6 mm. First, a hysteresis loop of the substrate and holder was measured and the saturation magnetization (M_s) was found to be about 4×10^{-4} emu, which was one or two orders of magnitude lower than that of the Fe–Pt multilayer films. Then the hysteresis loops of the Fe–Pt multilayers were measured, and the magnetization of the substrate and holder was subtracted automatically by the computer. To reduce the experimental error, measurements were made on an assembly of five similar specimens. Consequently, the magnetic moment from the substrate and holder had a negligible effect on the measured values, and the precision of the measured magnetic moment of the films was estimated to be better than 1%. After measuring the magnetic properties, the films were dissolved in 5 ml aqua ($HNO_3:HCl = 1:3$) and the Plasma-Spec-I inductive coupled plasma (ICP) atomic emission spectrum was employed to determine the Fe and Pt content in the multilayers. An average magnetic moment per Fe atom was then obtained using these data. Assuming the error involved in the ICP measurement to be 5%, the total error was around 6%.

3. Results and discussion

Low-angle x-ray diffraction analysis was used to verify the periodicity in Fe–Pt multilayers. Experimental results indicated that the periodicity of the films was exactly the thickness of Fe–Pt bilayers, and agreed well with the nominal values. For example, figure 1(a) shows a typical low-angle x-ray diffraction pattern of the [Fe (5.6 nm)–Pt (7.0 nm)]$_{12}$ films (the subscript is the number of Fe–Pt bilayers). From this pattern, six diffraction peaks of the Fe–Pt multilayer can clearly be seen, and the modulation periodicity, according to these data, is calculated to be 12.6 nm. Similar results of such periodicity can also be determined
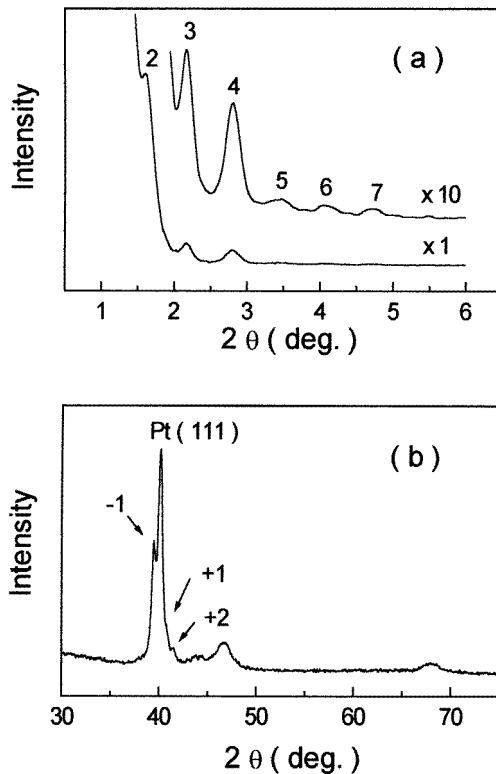
Figure 1. (a) The low- and (b) the high-angle x-ray diffraction patterns of [Fe (5.6 nm)–Pt (7.0 nm)]$_{12}$ multilayers.

from the satellite peaks of Pt(111) in a high-angle x-ray diffraction pattern for the same film (figure 1(b)). These patterns show that the sample has a periodic structure along the normal to the film plane.

To exclude possible errors in determining the thickness of the deposited metal layers from measuring the periodicity, RBS analysis was carried out to determine the total thickness and the average periodicity of the films. Figure 2 shows an RBS spectrum of an [Fe (8.0 nm)–Pt (7.0 nm)]$_{10}$ multilayer film as an example. This spectrum was obtained with 2.023 MeV He$^+$ ions, and the laboratory backscattering angle was 165°. In order to resolve individual layers by the detector at this energy, which presented a resolution of about 10 nm, the sample was tilted by 60°. From this spectrum, one can see that the peak corresponding to the high channel is from the platinum and the low channel is from the iron. Both iron and platinum signals consist of ten peaks, corresponding to ten Fe–Pt bilayers in the film. The total thickness of the sample is estimated to be about 150 nm by resolving the RBS spectrum, which agrees with the nominal thickness.

The microstructure of the films was investigated by x-ray diffraction, HEEM and SAD analysis. Figure 3 shows the x-ray high-angle diffraction patterns of Fe–Pt multilayer films. From this figure, one can see that when $t_{Fe} < 3.4$ nm, there is only one fcc phase, and its lattice parameter is about 0.389 ± 0.002 nm, which is slightly smaller than that of pure Pt, i.e., 0.392 nm. When t_{Fe} reaches 5.6 nm, a bcc Fe(110) diffraction line emerges, indicating that the bcc Fe phase is formed in the films.
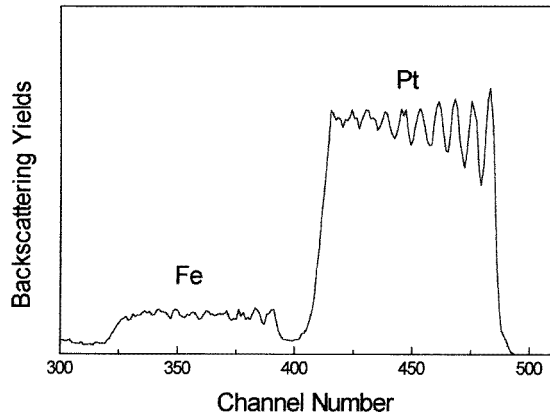
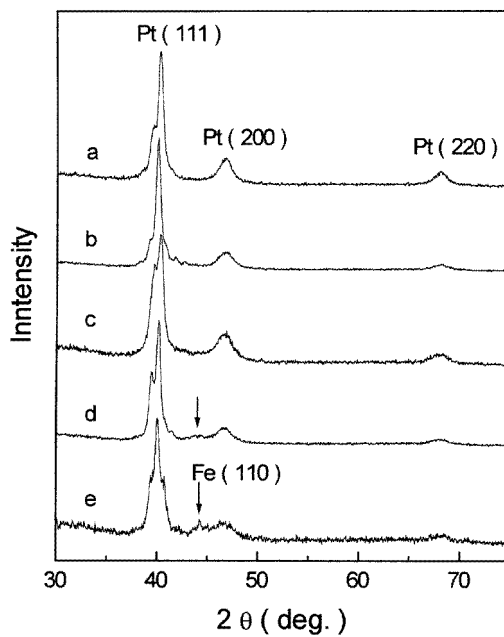**Figure 2.** The RBS spectrum of the [Fe (8.0 nm)–Pt (7.0 nm)]$_{10}$ multilayers.

Figure 3. The x-ray diffraction patterns of Fe–Pt multilayers with t_{Fe} increasing: a, [Fe (1.2 nm)–Pt (7.0 nm)]$_{18}$; b, [Fe (2.3 nm)–Pt (7.0 nm)]$_{16}$; c, [Fe (3.4 nm)–Pt (7.0 nm)]$_{14}$; d, [Fe (5.6 nm)–Pt (7.0 nm)]$_{12}$; e, [Fe (8.0 nm)–Pt (7.0 nm)]$_{10}$.

There are two possible mechanisms for the formation of only one fcc phase in Fe–Pt multilayers with Fe layers thinner than 3.4 nm. Firstly, the Fe atoms might grow in an fcc structure on the polycrystalline fcc Pt layers. Secondly, an fcc solid solution might be formed at the Fe–Pt interfaces. According to RBS and low-angle x-ray diffraction results, the films had a good periodic structure, and the lattice parameter of the observed fcc phase was about the same as that of pure platinum. It could therefore be thought that, in our experimental conditions, the growth of Fe atoms in an fcc structure on the thick Pt layers is responsible for observing only one fcc structure phase. When $t_{Fe} > 5.6$ nm, the Fe can not

grow in an fcc structure on the Pt layer because of the internal stress caused by the large mismatch between Fe and Pt, which is about 8%, resulting in the formation of bcc Fe in these films, shown in figure 3. HEEM SAD polycrystalline diffraction patterns presented in figure 4 also reveal the same results. From this figure, one can see that some texture occurs in [Fe (2.3 nm)–Pt (7.0 nm)]$_{16}$ samples, which is similar to our previous observation in Fe–Ag multilayers [14].

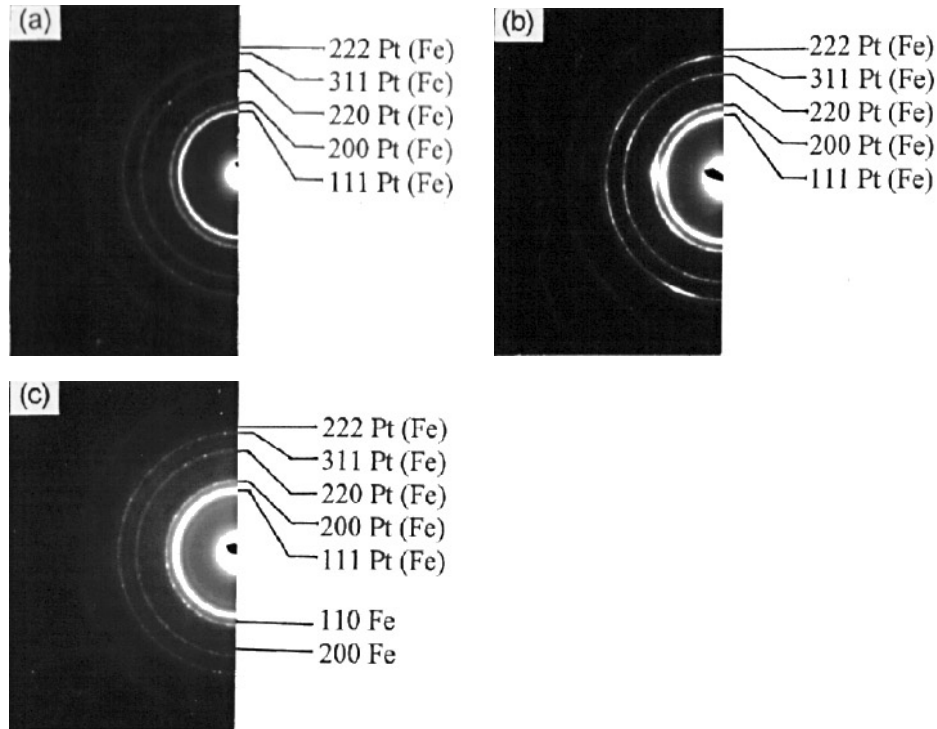**Figure 4.** Electron diffraction patterns of the Fe–Pt multilayers: (a), [Fe (1.2 nm)–Pt (7.0 nm)]$_{18}$; (b), [Fe (2.3 nm)–Pt (7.0 nm)]$_{16}$; (c), [Fe (8.0 nm)–Pt (7.0 nm)]$_{10}$.

Figure 5 shows the hysteresis loops of Fe–Pt multilayers in a magnetic field of up to 10 kOe parallel to the film plane. Figure 6 shows the average magnetic moment per Fe atom in Fe–Pt multilayered films as a function of t_{Fe}. From figures 5 and 6, one can see that all the Fe–Pt multilayers, including films with fcc Fe, are ferromagnetic and have an in-plane easy axis of magnetization. For [Fe (2.3 nm)–Pt (7.0 nm)]$_{16}$ multilayers, the magnetic moment per Fe in the fcc structure reaches a highest value of $2.12\mu_B$, which is about the same as that in bulk bcc Fe ($2.15\mu_B$). In other words, these results show that Fe atoms in an fcc structure can behave ferromagnetically with a high magnetic moment.

In our recent work concerning Fe–Cu and Fe–Pd nano-multilayers [3, 12], it was found that, when the Fe layers were very thin, fcc Fe with a lattice parameter of 0.360 ± 0.005 nm could be formed, and the fcc Fe, in both Fe–Cu and Fe–Pd systems, exhibited ferromagnetism and an enhanced magnetic moment per Fe atom, i.e., the maximum value was $3.44\mu_B$ for Fe (1.5 nm)–Cu (7.5 nm) films and $3.27\mu_B$ for Fe (1.6 nm)–Pd (6.5 nm) films. This is significantly higher than that in Fe–Pt multilayers, which is only $2.12\mu_B$. The main reason for the observed difference in magnetism in the Fe–Pt, Fe–Cu, and Fe–Pd multilayers may be the following. For both Fe–Cu and Fe–Pd systems, the fcc
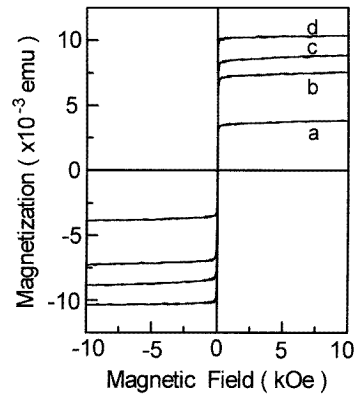
Figure 5. The hysteresis loops of Fe–Pt multilayers: a, [Fe (1.2 nm)–Pt (7.0 nm)]$_{18}$; b, [Fe (2.3 nm)–Pt (7.0 nm)]$_{16}$; c, [Fe (3.4 nm)–Pt (7.0 nm)]$_{14}$; d, [Fe (8.0 nm)–Pt (7.0 nm)]$_{10}$.
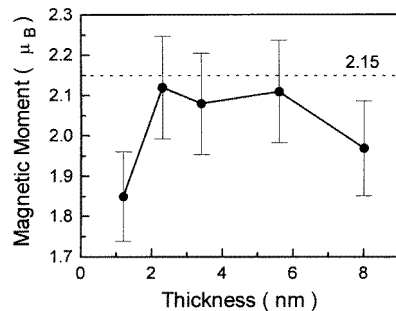

Figure 6. Magnetic moment of Fe–Pt multilayers as a function of t_{Fe} when $t_{Pt} = 7.0$ nm.

Fe had a similar lattice parameter (around 0.360 nm), which could be considered as an ideal situation used in theoretical investigations. However, for Fe–Pt multilayers, the fcc Fe had a lattice parameter of 0.389 ± 0.002 nm, which was larger than that in Fe–Cu and Fe–Pd films. Moruzzi *et al* [15] calculated the total energy and magnetization of bulk fcc iron, and pointed out that the magnetism is related to the Wigner–Seitz radius, which contains the same volume as that of an atom in the actual lattice. The Wigner–Seitz cell volume of the fcc Fe in the Fe–Pt films is 20–30% greater than that in the Fe–Cu and Fe–Pd films, and this results in a smaller magnetic moment per Fe atom in the Fe–Pt films. This may give a possible explanation for the observed magnetic properties of fcc Fe in the Fe–Pt nano-multilayers. It is also seen that, even though Fe can grow with an fcc structure in various systems, the magnetic properties of fcc Fe changes with the lattice parameter of the fcc Fe phase, which depends on the other metals in the system. From figure 6, one can also see that the magnetic moment per Fe atom in various cases was lower than that of bulk Fe ($2.15\mu_B$). The magnetic moment slightly increased with decreasing t_{Fe}, reaching a highest value of $2.12\mu_B$ when $t_{Fe} = 2.3$ nm, and then it decreased with decreasing t_{Fe}.

Figure 7 shows two hysteresis loops of Fe–Pt multilayers measured in the magnetic field perpendicular to the film plane. It is seen that the normalized magnetization, for the perpendicular case, depends on the t_{Fe}, when $t_{Pt} = 7.0$ nm. Magnetization of the [Fe (2.3 nm)–Pt (7.0 nm)]$_{16}$ multilayers was easier than that of [Fe (8.0 nm)–Pt (7.0 nm)]$_{10}$
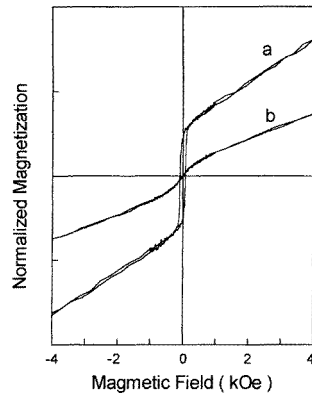
Figure 7. The hysteresis loops of Fe–Pt multilayers in a magnetic field perpendicular to the film plane for [Fe (2.3 nm)–Pt (7.0 nm)]$_{16}$ (a) and [Fe (8.0 nm)–Pt (7.0 nm)]$_{10}$ (b).

ones. This revealed that there is an increasing tendency for perpendicular magnetization in the Fe–Pt multilayers when t_{Fe} decreases, which is similar to our previous observations in Fe–noble-metal multilayers [3, 12].

4. Conclusions

In summary, we have shown that fcc iron in Fe–Pt multilayers exhibits ferromagnetic behaviour, and its magnetic moment can be as high as $2.12\mu_B$ in [Fe (2.3 nm)–Pt (7.0 nm)]$_{16}$ films. Such properties, to our knowledge, have not been reported previously. The magnetic moment per Fe atom in an fcc structure in Fe–Pt films is smaller than those observed in the Fe–Cu and Fe–Pd films (3.44 and $3.27\mu_B$ respectively), which is probably correlated with the lattice parameter of metastable fcc phase iron, i.e., a large lattice parameter results in a decrease of magnetic moment in thin films.

Acknowledgments

References

[1] Freeman A J and Wu R 1992 *J. Magn. Magn. Mater.* **104–107** 1
[2] Krompiewski S, Krauss U and Krey U 1991 *J. Magn. Magn. Mater.* **92** L295
[3] Liu B X and Pan F 1993 *Phys. Rev.* B **48** 10 276
[4] Freeman A J and Fu C L 1987 *J. Appl. Phys.* **61** 3356
[5] Fu C L, Freeman A J and Oguchi T 1985 *Phys. Rev. Lett.* **54** 2700
[6] Wimmer E, Freeman A J and Kradauer H 1984 *Phys. Rev.* B **30** 3113
[7] McHenry M E and MacLaren J M 1991 *Phys. Rev.* B **43** 10 611
[8] MacLaren J M, McHenry M E, Crampin S and Eberhart M E 1990 *J. Appl. Phys.* **67** 5406
[9] Tersoff J and Falicov L M 1982 *Phys. Rev.* B **26** 6186

[10] Falicov L M, Victora R H and Tersoff J 1985 *The Structure of Surfaces* ed M A Van Hove and S Y Tong
       (Heidelberg: Springer) p 12
[11] Pan F, Yang T and Liu B X 1995 *Phys. Status Solidi* a **149** 677
[12] Pan F, Yang T, Zhang J and Liu B X 1993 *J. Phys.: Condens. Matter* **5** L507
[13] Koide T, Shidara T, Yamaguchi K, Fujimori A, Fukutani H, Nakajima N, Sugimoto T, Katayama T and
       Suizuki Y 1996 *Phys. Rev.* B **53** 8219
[14] Pan F, Yang T, Tao K and Liu B X 1992 *J. Phys.: Condens. Matter* **4** L519
[15] Moruzzi V L, Marcus P M, Schwarz K and Mohn M 1986 *Phys. Rev.* B **34** 1784